REVIEW OF WATERFORD III BASEMAT ANALYSIS

Structural Analysis Division

Department of Nuclear Energy

Brookhaven National Laboratory

Upton, NY 11973

July 18, 1984

TABLE OF CONTENTS

ABSTRACT

The Structural Analysis Division of the Department of Nuclear Energy at BNL undertook a review and evaluation of the Waterford III basemat. Based upon a review of the detailed finite element analyses performed by Harstead Engineering Associates on behalf of the applicant, together with approximate analyses developed by BNL, it is concluded that the observed cracks developed on the top surface of the mat during the construction phase and were most probably caused by differential settlement induced by the dead loads acting alone or by dead loads acting on a mat already cracked by normal thermal and/or shrinkage effects. For this latter case, the bending induced in the mat by the dead loads would cause these cracks to open and become larger. In the latter stages of construction, when the backfill was in place and the water table restored to its natural level, additional loadings caused by the side wall soil and water pressures offset these effects.

All of the approximate check calculations performed by BNL confirm these conclusions and, together with engineering judgment, lead to the conclusion that the safety margins in the design of the mat are adequate. The BNL calculations also indicate that the development of cracks in the basemat due to diagonal tension, either from the applied dead loads or from any potential differential settlements between blocks during construction, is unlikely. The cracks that have appeared in the vertical walls do not alter these conclusions and do not appear to present a significant safety issue. Nonetheless, it is recommended that some

detailed confirmatory calculations be performed, although it is not anticipated that these analyses will lead to any substantial differences in the results. In addition, it is recommended that a surveillance program be initiated to monitor tne cracks.

INTRODUCTION

At the request of the NRC Staff, the Structural Analysis Division of the Department of Nuclear Energy at BNL undertook a review and evaluation of the HEA Waterford III mat analysis documented in Harstead Engineering Associates (HEA) Reports, Nos. 8304-1 and 8304-2. Both reports are entitled "Analysis of Cracks and Water Seepage in Foundation Mat." Report 8304-1 is dated September 19, 1983, while Report 8304-2 is dated October 17, 1983. Major topics addressed in the first report are:

(1) Engineering criteria used in the design, site preparation and construction of the Nuclear Plant Island Structure basemat.

(2) Discussion of cracking and leakage in the basemat.

(3) Laboratory tests on basemat water and leakage samples.

(4) Stability calculations for the containment structure.

The second report concentrates on the finite element analysis and its results. Specifically, it describes:

(1) The geometric criteria and finite element idealization.

(2) The magnitude and distribution of the loads.

(3) The final computer results in terms of moments and shear versus the resistance capacity of the mat structure.

Supplemental information to these reports was obtained at meetings held in Bethesda, MD, on March 21, March 26, and July 3, 1984; at the Waterford plant site in Louisiana on March 27, 1984; and at Ebasco headquarters in New York City on April 4 and July 2, 1984. At the close of the EBASCO meeting on April 4, 1984, a complete listing of the HEA computer run was made available to BNL.

The BNL efforts were originally concentrated on a review of the results presented in HEA Report No. 8304-2 and on the supplemental information contained in the computer run given to us by HEA. This computer run contains the nine design load cases and their various combinations. The input/output printout consists of roughly two thousand pages of information. Selected portions were reviewed in detail, while the remaining sections were reviewed in lesser detail.

As a result of further discussions with the NRC Staff, the BNL workscope was expanded to include the following additional topics:

a) East-West cracks internal to the shield wall

b) Average vertical shear

c) Punching shear

d) Stresses resulting from pouring adjacent mat blocks

e) Effect of sidewall loads on basemat capacity

f) Shear margin for mat areas located between column lines (9M to 12A) and (R to Q_1)

g) Cracks in the vertical walls of structures placed on the basemat.

Comments regarding this work are given in the sections that follow.

GENERAL COMMENTS

Basically, the HEA report concludes that bending moments will produce tension on the bottom surface of the mat in the final as-built condition (backfill in place and water table restored to its natural elevation). For this condition, including required seismic loading, it is shown that the design is conservative. Furthermore, the shear margin

(shear capacity vs. the shear produced by load combinations) is concluded by HEA to be adequate although a few elements were found to be close to the design capacity. Accordingly, the cracking of the top surface is attributed by HEA only to "benign" causes such as shrinkage, differential soil settlement, and temperature changes.

Based on the discussions held with EBASCO and HEA, and on the review of data given to BNL, it is our judgment that the bottom reinforcement as well as the mat shear capacity is adequate. The statement that the cracking of the top surface is attributable to "benign" causes, however, was not analytically demonstrated by HEA. In the BNL review of the reports and data, an attempt was made to ascertain the reasons for the existing crack patterns that appear around the outside of the reactor shield building as depicted in Figure D-I, Appendix D, of HEA Report No. 8304-2. Other effects influencing the structural behavior and safety were also investigated. Specifically, the structural analysis topics reviewed in more detail include:

(1) Dead loads and their effects.

(2) East-West cracks internal to the shield wall.

(3) Buoyancy forces and their effects.

(4) Variable springs used for the foundation modulus.

(5) Vertical earthquake effects.

(6) The side soil pressures.

(7) The boundary constraint conditions used for the mat.

(8) Finite element mesh size and its effects.

(9) Average vertical shear.

(10) Punching shear.

(11) Stresses resulting from pouring adjacent mat blocks.

(12) Effect of sidewall loads on basemat capacity.

(13) Shear margins for mat areas located between column lines (9M to 12A) and (R to Q_1).

(14) Cracks in vertical walls of structures placed on the base mat.

STRUCTURAL ANALYSIS TOPICS REVIEWED

1. Dead Loads (D)

As mentioned, EBASCO in its discussion, and HEA in its reports, have not shown analytically the cause of the top surface cracks. In reviewing the HEA computer outputs, it was found that element moments and shears for individual loadings are explicitly given. These individual loadings are factored together at the end of the computation to provide the overall combined loading calculations. Since individual loading conditions were explicitly given, BNL extracted certain information from these computer runs to provide an assessment of the contribution of the various loading conditions to calculated stresses. Thus, for the case involving dead loads only, a number of elements in the regions where the principal surface cracks appear exhibit moments (positive in sign) that can produce tension and thus create cracking on the top surface. This situation is shown in Table 1 which gives moment data (M_x, M_y and M_{xy}) for elements under various load conditions (dead (D), bouyancy (B) and normal side pressure) in the regions which generally correspond to the areas where the principal surface cracks appear (compare Fig. 1 to Fig. 2).

TABLE 1

	ELEMENT	Mx (kip-ft/ft) D	Mx (kip-ft/ft) B	My (kip-ft/ft) D	My (kip-ft/ft) B	Mxy (kip-ft/ft) D	Mxy (kip-ft/ft) B	Normal Side Pressure Mx	Normal Side Pressure Mx	Normal Side Pressure Mxy
Area T2-R-12M-7FH	437	-242	173	-574	197	116	- 31	-294	-196	93
	212	655	595	207	91	106	- 25	-663	-392	79
	211	-605	205	-412	217	-296	48	-219	-416	- 76
	207	64	99	-136	136	- 81	15	-319	-193	50
	441	-105	168	172	-170	39	- 12	-347	-489	66
	436	-719	269	-1193	357	531	-130	-274	-258	117
	438	269	142	-159	158	- 60	26	-730	-347	27
	447	665	59	210	88	248	- 55	-653	-339	-127
	204	193	87	569	72	-143	28	-361	-420	24
	208	350	32	898	- 24	-241	75	-354	-771	- 49
	203	-676	260	-995	236	39	- 21	-574	-247	30
	426	-542	157	-705	310	332	- 65	-171	-486	61
Area R-P-2M-1A	259	62	148	-133	81	154	- 36			
	253	5	71	531	75	0	18			
	255	30	58	670	5	41	10			
	252	86	24	611	- 55	87	8			
	254	50	26	412	- 41	69	9			
	251	37	5	162	- 23	44	12			
	257	320	- 38	57	15	- 81	- 15			
	248	255	- 26	29	16	- 29	- 6			
	267	-236	80	87	118	- 64	28			
	269	-173	59	434	10	- 82	32			
Area R-P1-12A-9M	419	-314	137	-635	313	- 30	12			
	410	-371	71	-642	238	270	- 29			
	400	-315	108	-774	275	- 44	41			
	401	-180	42	-201	102	108	- 23			
	414	-304	118	-130	178	44	- 19			
	417	-200	93	440	41	- 17	- 15			
	404	- 64	17	428	- 32	98	- 18			

NOTE: D - Dead Load

B - Bouyancy

+ M causes tension at the top surface of the mat.

- M causes tension at the bottom surface of the mat

x = moment along north-south orientation of mat

y = moment along east-west orientation of mat

xy = twisting moment

kip = 1000 lbs.

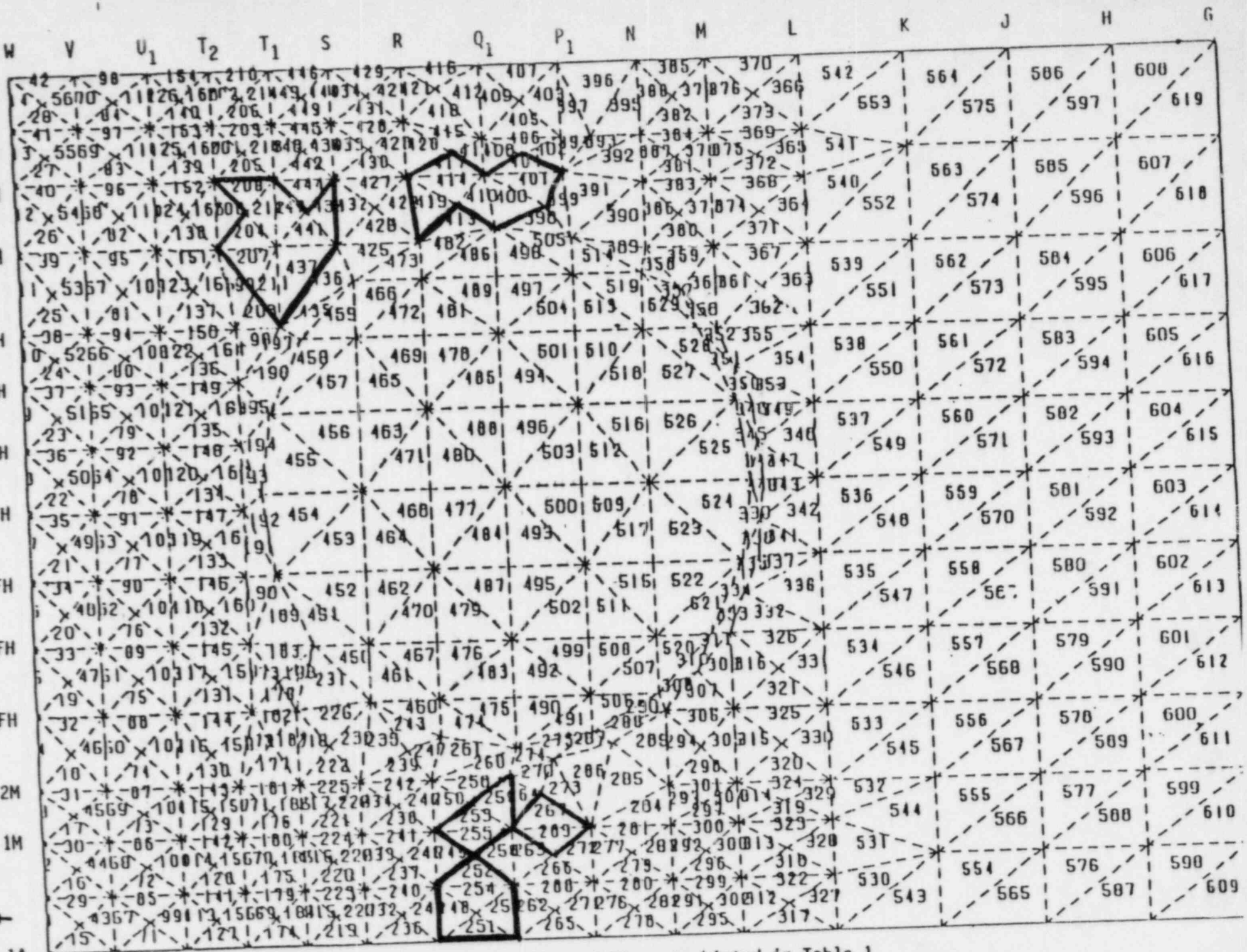

Fig. 1 Location of Elements Listed in Table 1.

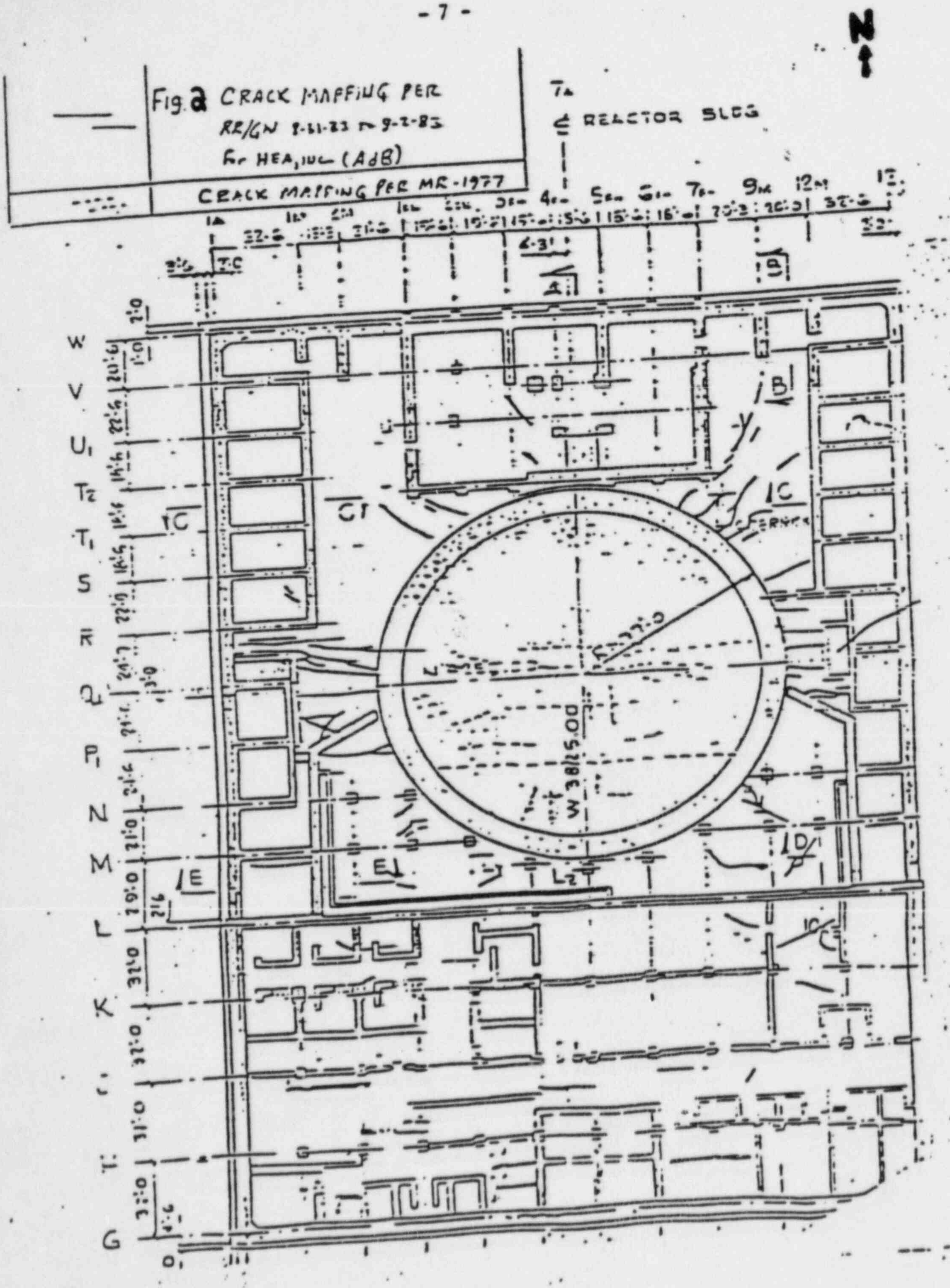
Fig. 2 CRACK MAPPING PER
RR/GN 8-31-83 to 9-2-83
For HEA, INC (AdB)
CRACK MAPPING PER MR-1977
℄ REACTOR BLDG
N
W
V
U1
T2
T1
S
R
Q
P1
N
M
L
K
G
W 38/25.00

Prior to discussing the results shown in Table 1, it is necessary to consider the strength characteristics of the base mat. In particular, the bending moments causing tensile stresses in the top of the mat are of interest. As may be seen from Figure 3, all of the north-south reinforcement for the top of the mat consists of No. 11 bars placed six inches on center (#11 @ 6"). The top east-west reinforcement is also #11 @ 6" except in the vicinity of the containment where #11 @ 12" are added.

Table 2 gives approximate values of the bending moment required for the two reinforcement patterns utilized in the top of the mat, (a) to cause the steel to reach an allowable stress of 24 ksi (ACI Code working stress capacity), (b) to crack the concrete, (c) to yield the top reinforcement, and (d) to reach the ultimate moment capacity of the section.

TABLE 2

BENDING MOMENT REQUIRED TO:	TOP REINFORCEMENT #11 @ 6"	TOP REINFORCEMENT #11 @ 6" + #11 @ 12"
Reach working stress capacity (in steel)	820 kips-ft/ft	1230 kips-ft/ft
Crack the concrete	1640	1640
Yield top reinforcement	1360	2040
Reach ultimate capacity	1480	2220

CLIENT LOUISIANA POWER & LIGHT CO
PROJECT WATERFORD S.E.S. UNIT NO 3
SUBJECT COMMON PDN MAT + REINF

JOB NO. _____ DEPT. NO. _____
BY _____ DATE _____
CHECKED BY _____ DATE _____

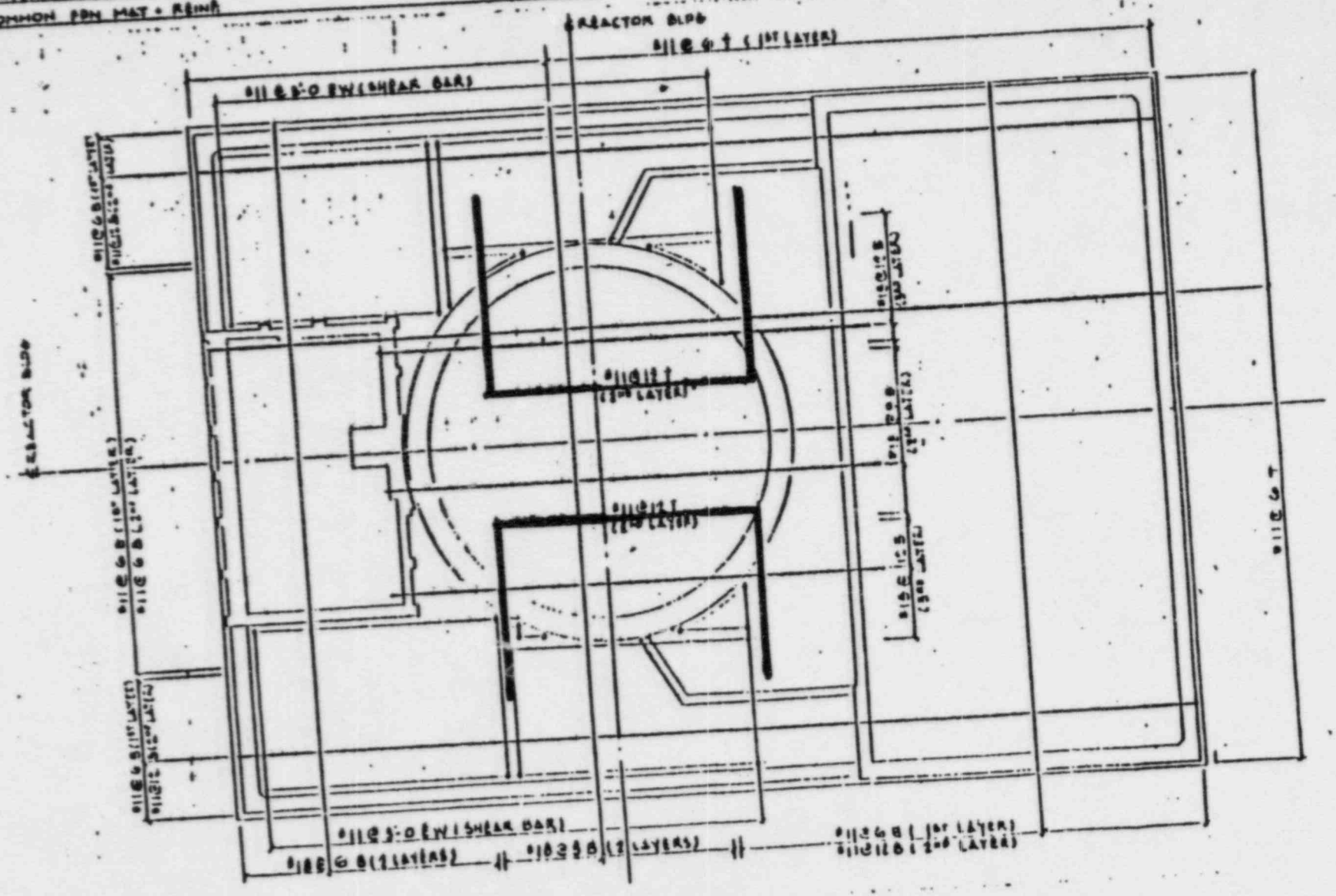

Fig. 3 MAT REINFORCEMENT

Table 2 indicates that bending moments of less than 1640 kip-ft/ft would not cause cracks to occur in a section of the basemat which had no existing cracks. However, if some cracks already existed in the mat (as undoubtedly would be the case because of temperature and shrinkage effects), one would expect the existing cracks to become more pronounced when the bending moment approached the working stress capacity of the top steel (820 kip-ft/ft for the more lightly reinforced section, and 1230 kip-ft/ft for the more heavily reinforced section).

Returning to the data shown in Table 1, it is to be noted that the moments in several elements exceed the working stress capacity. For example, for element 208, the dead load (D) moments M_x and M_y are respectively equal to 350 and 895 kip-ft/ft and are positive. Thus, as mentioned previously, the top surface of the mat in this area is in tension. The maximum principal moment is a function of M_x, M_y, and M_{xy} and its computed value is close to 1000 kip-ft/ft. This moment exceeds the working stress capacity and thus would be expected to expand any existing shrinkage and thermal cracks in this element. Similarly, any such pre-existing concrete cracks would become more significant under the dead load condition in other elements located in the three areas where major cracking in the basemat outside the shield wall was observed, i.e., elements 447, 212, 204, 253, 255, 269, 257, 417, and 404 (see Figure 2).

Thus, the cracks on the top surface of the mat outside the shield wall would be expected to have occurred after construction of the superstructure, but before placement of the backfill. It should be noted that there was, in fact, no period in which the superstructure was fully completed before the backfill was placed and before the ground water was allowed to rise and exert a buoyancy effect, i.e., the condition modeled by the "dead load" calculations. However, based on information provided in discussions with EBASCO and HEA personnel, there was a period before dewatering was stopped and before the backfill was placed when a substantial portion of the superstructure was in place; the shield wall was virtually completed and many of the side walls and internal structures were in place.* Thus, while there is no explicit computation of loading conditions at this point in the construction of the facility, the dead load portion of the HEA finite element analysis provides a reasonable simulation of the actual loading to permit a conclusion as to the probable cause of the surface cracking.

In view of the comments made in section 8 of this report, regarding the finite element grid size used by HEA and EBASCO in their analysis and the effect of this grid size on the accuracy of the analysis, an approximate analysis of a strip of the mat was made by BNL. This strip was taken at the center of the reactor building in the N-S direction with a width of 22 ft. In this analysis, the mat was considered to be infinitely stiff (a conservative assumption) and subjected to the dead loads taken from the HEA computer input. The maximum moment for this case occurs close to the center of the reactor and results in tension

on the top surface of the mat. While this analysis admittedly is conservative, it supports the previous conclusion that cracking could have occurred during construction due to tensile bending stresses in the top of the mat. Similar results would be found at the other cracked sections shown shaded in Fig. I.

In summary, the cracking on the top surface of the mat is most probably caused by dead loads acting on elements already cracked due to normal thermal and shrinkage effects. The dead load moments would enhance previously existing small and most likely unobservable cracks, causing them to become larger and observable.

2. East-West Cracks Internal to the Shield Wall

As shown in Fig. 2, crack patterns were also noted in March 1977, internal to the shield wall. At that time, based on information provided by EBASCO, the shield wall was partially constructed up to elevation 187' and the steel containment was supported on temporary footings. Other walls or structures on the mat either were not yet constructed or were only partially constructed. Since the computer dead load calculations refer to the mat with all existing structures, which of course has different dead weight loads and different spatial distribution of these loads than the partially completed case (for example, the massive concrete fill on which the containment rests, plus all equipment in containment, would not be included in a model of the 1977 configuration), it is not possible to utilize the HEA computer results to explain the

1977 cracks. It is noted, however, that the additional top reinforcements (i.e., # 11 @ 12" as shown in Fig. 3) are essentially located in areas under the shield wall and are placed in an east-west direction. Thus, if cracking should occur, the preferred direction would be parallel to the direction of the heavier reinforcement, or east-west in orientation. This is indeed the direction of the cracks, and these cracks, in all likelihood, had the same origins as the cracks outside the shield wall (dead loads acting in conjunction with thermal and shrinkage effects).

The additional east-west direction top reinforcements will also cause prevailing cracks in elements located outside the shield wall circle, directly east and west to the shield wall (i.e., those shown shaded in Fig. 1 in areas R-P-2M-1A and R-P1-12A-9M) to be oriented in an east-west direction. This is indeed the pattern indicated in Fig. 2. In contrast, since there is no additional top reinforcement in the elements shown shaded in Fig. 1 located between sections T2-R-12M-7FH (in the northeast sector of the mat), the prevailing cracks do not necessarily have to be oriented in the east-west direction.

3. Buoyancy Forces (B)

The moment results from our analysis (Table 1) show that these forces when acting alone would mostly cause tensile stress on the top surface of the mat. The moments causing these stresses are tabulated in Table 1 under the column heading B for groups of elements in the identified cracked regions of the mat. As can be seen, these moments are not as severe as those due to dead weight. By superposition they could in

some cases contribute to higher tensile stresses and thus result in further cracking in some areas of the top surface of the mat.

4. Variable Springs Used for the Foundation Modulus

Moments and shears developed in the basemat were computed using the concept of the Winkler foundation; namely, the soil is represented as a series of relatively uniform independent springs. The stiffness of the springs is obtained from approximate analyses which are based on generalized analytical solutions available for rigid mats on the surface of elastic soils. The actual design of the mat was based on a series of iterative computer runs in which the soil stiffness was varied until the computed contact pressures under the mat were fairly uniform and equal to the overburden stress at the elevation of the foundation mat. This approach appears to be reasonable when assessing the final stress conditions. Long term consolidation effects can be anticipated to cause effective redistribution of loads and cause the mat to behave in a flexible manner. However, during the initial loading stages this approach is not applicable since load redistribution is continuously taking place.

5. Vertical Earthquake Effects

Vertical earthquake effect was not discussed in the HEA reports. However, from the finite element analysis printout and conversation with HEA engineers, it was stated by HEA and EBASCO that this effect was included in the load combination cases by specifying an additional factor of 0.067, which was then applied to the dead and equipment load case.

From these discussions and our review, it is not clear to BNL whether an amplification factor due to vertical mat frequency was or was not used.

In order to obtain a rough estimate of this effect, the north-south direction of the mat was simulated by a beam on fourteen elastic supports. The total weight of the mat, the superstructure, the equipment, etc., as well as the spring constants, were the same as those used by Ebasco and HEA in their computer run. The natural frequencies obtained from this analysis are shown below in Table 3.

Table 3

Natural Frequencies of Simulated Mat

Mode Number	Frequency (Cycles/sec)
1	.4557E+01
2	.5308E+01
3	.5753E+01
4	.5923E+01
5	.6210E+01
6	.7035E+01
7	.8007E+01
8	.1058E+02
9	.1295E+02
10	.1769E+02
11	.2009E+02
12	.2461E+02
13	.3248E+02
14	.3752E+02

As can be seen from Table 3, the frequencies vary from 4.56 to 37.52 cps (i.e. .4557E+01 to .3752E+02). Using Regulatory Guide 1.60, for the 5% damping case, it is found that amplification factors for these

frequencies will vary from 3.0 to 1.0. For the first seven frequencies shown in Table 2, the amplification factors will be less than 3.0 but above 2.60. From the review it seems that the vertical amplification factor used by HEA was 1.34, which is below 2.60. It should be realized, however, that not all response parameters (moments, shears, etc.) are equally affected by the natural frequencies of the mat. Moreover, the frequencies were obtained from a simplified model. Hence, to apply an overall amplification factor of even 2.5 to all response parameters is not reasonable. The flexibility of the mat generally will result in some local increases in the computed seismic moments at some particular locations. Where this increase occurs is hard to ascertain without performing a very detailed dynamic analysis. Since the effects are localized, we believe that they should not greatly influence the gross resultant forces acting on the mat. However, a proper dynamic analysis should be performed to verify the stresses which may be expected to result.

6. Side Soil Pressure

According to the STARDYNE computer results obtained from HEA, the normal side soil pressures produce large moments that are opposite to those caused by the dead loads, as shown in Table 1 where moments of elements located in one of the cracked regions outside of the shield building (T2-R-12M-7FH) are compared. The total moments in some cases (e.g., elements 447 and 208) become quite small. In other regions, there is a reversal of the total bending moment, resulting in tension on the bottom surface and compression on the top. This compression would tend

to close the cracks on the upper surface. Thus, it appears that side soil pressure is an important load case for the mat design.

For the static or normal operating condition, the lateral pressures are based on the at-rest stress condition and are uniform around the periphery of the structure. For the seismic problems the pressures are computed to approximately account for relative movements between the structure and the soil. On one side, the structure will move away from the lateral soil (active side) and reduce the pressures, while the opposite will occur on the other side (passive side). The actual computations by EBASCO made use of actual site soil properties to arrive at the soil pressures, rather than the standard Rankine analyses. No dynamic effects on either the lateral soil or pore pressures were included. The sensitivity of the calculated responses to these effects are currently unknown. However, approximate estimates of these dynamic effects made by BNL indicate that the total lateral load should change by no more than 15 per cent. Nonetheless, a proper analysis including dynamic effects should be performed to verify this result.

7. Boundary Constraints

For equilibrium calculations no special consideration need be made for the vertical case since the soil springs prevent unbounded structural motion. However, the same cannot be said for the horizontal case since soil springs are not used to represent the soil reactions. Rather, the lateral soil forces are directly input to the model. To prevent unbounded rigid body motion, artificial lateral constraints must be imposed on the

model. The constraints are depicted in Fig. 4. The nodes shown circled were constrained from movement in the y (east-west) direction, while those described by "x" were constrained in the x (north-south) direction. As is commonly practiced in finite element applications, the constraints are placed in a manner that they do not overly affect the static and dynamic response calculations. From the output presented in the EBASCO and HEA reports, this effect was not evaluated. The stresses caused by the artificial boundaries should be calculated and compared with those presented.

8. Finite Element Mesh and its Effects

In general, finite element models for plate structures require at least four elements between supports to obtain reasonable results on stress computations. The models used by both EBASCO and HEA violate this "rule of thumb" in the vicinity of the shield wall. The significance of this effect is demonstrated in Figure D-3 of Report No. 8304-2 which presents a plot of moment taken through the center of the slab. The computed moments in adjacent elements 193, 194 and 455 are -3800, -2500 and +400K. The elements used in the HEA analysis are constant curvature elements so that the computed moments will be constant within each element. The steep moment gradient between the elements indicates that a finer mesh would be advisable. A similar effect was also noted when investigating the elements forming the junction between the lateral earth retaining walls and the base mat. Finally, in order to obtain a better approximation of the shear and bending moments within an element (with less oscillation about the true solution), quadrilateral elements are recommended for the mat analysis.

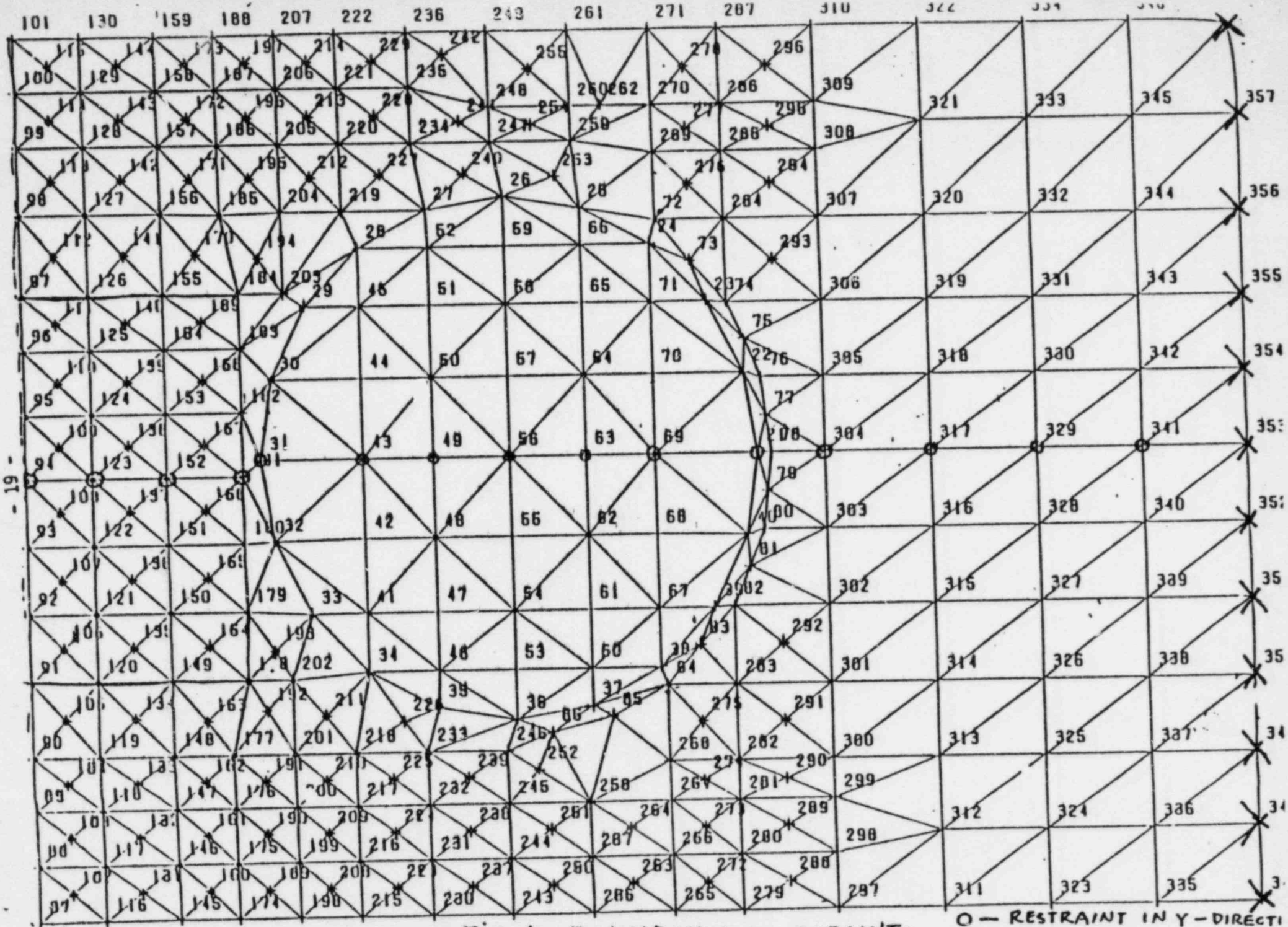

FIG 4 BOUNDARY CONSTRAINTS

9. Average Vertical Shear

Several elements in the Ebasco/HEA analysis indicate local areas where allowable shear stresses are exceeded. However, shear failure should not be associated with local exceedance of an allowable shear stress, because the loads are distributed across the entire potential failure plane. All of the ACI code shear requirements are based on this approach. Average vertical shear stresses (i.e., diagonal tension) were computed by BNL in the base mat for two sections across the mat; one section is in the E-W direction and the other in the N-S direction. These sections were chosen to include those elements which indicated high shear stresses in the HEA analysis and where actual cracking was noted. The highest average shear stress computed for any design load combination is 50 psi. The allowable shear stress for this case, in accordance with Chapter 11 of ACI Standard 318-77, is 107 psi ($2\phi\sqrt{f'_c}$). Thus, a safety factor of greater than two is available to prevent shear failure under the design load combination.

10. Punching Shear

Another potential failure surface in the base mat considered by BNL is a punching shear section located a distance of d/2 outside the reactor shield wall, as recommended in Chapter 11 of ACI Standard 318-77. The peak value of shear stress due to both SSE overturning moments and normal operating loads (plus proper load factors) were close to but always less than the allowable design shear ($4\phi\sqrt{f'_c}$).

11. Stresses Resulting From Pouring Adjacent Mat Blocks

BNL has explored the question of whether diagonal tension cracks may have occurred during the process of pouring adjacent mat blocks. To determine if such cracking could have occurred an approximate analysis was made, as set forth in Appendix B. The adjacent blocks are assumed to rest on foundation springs which represent the soil flexibility. The second block poured was assumed to harden instantaneously thereby overestimating the shear load carried by the first block due to relative settlement of the two blocks. As indicated in Appendix B, the resulting stresses were found to be sufficiently small so that neither diagonal tension stress, nor bending tensile stress alone, would be expected to cause cracking. Moreover, the likelihood of moment cracking was significantly greater than the likelihood for shear cracking. These conclusions are valid even for the case with soft spots in the foundation soils, i.e., where the soil modulus under one block is one-half that of the soil modulus under the adjacent block.

It should be noted that, according to EBASCO, soil settlement at the site was found to be instantaneous based on actual measured data. The concrete has almost no strength for the first eight to twelve hours and therefore even the small stresses calculated in Appendix B are unlikely.

12. Effect of Sidewall Loads on Basemat Capacity

Under normal operating conditions the loads acting on the side walls produce an average compressive stress in the base mat of about 50 psi. When seismic loads are included in this computation, the average

compressive stress in the base mat is reduced, but is still about 38 psi. These compressive stresses provide additional shear strength which have not been included in evaluating the capacity of the mat to carry diagonal tension stresses. It should be noted, as indicated in section 9 of this report, that the highest average shear stress developed in the base mat is only 50 psi. If this shear stress is combined with the 38 psi average compressive stress one finds that the diagonal tensile stress in the concrete is reduced to 34 psi. It is unlikely that this shear stress could cause a shear (diagonal tension) failure given the 107 psi shear capacity. This analysis is presented in Appendix C.

13. Shear Margins For Mat Areas Located Between Column Lines 9M to 12A and R to Q_I

In response to a request by the NRC Staff, EBASCO provided an estimate of peak diagonal tensile stress in a region bounded by column lines 9M-I2M-R-Q1 (Figure 1). EBASCO indicated that the average diagonal tensile stress, for the SSE case, in elements 410, 413, 414 and 419 was 210 kips/ft, as compared to a capacity of 274 kips/ft. A meeting was held at EBASCO on July 2, 1984 to review these data. The following conclusions were reached at that meeting:

(a) The EBASCO estimates of 210 kips/ft was overly conservative, for the following reasons. Two shears are associated with each of the elements. The first (F_{xz}) acts on a plane lying in the north-south direction, and the second (F_{yz}) acts on a plane lying in the east-west direction. The computer output gives these results in local element

coordinates rather than in global coordinates. EBASCO used the maximum value of either F_{xz} or F_{yz}, although these maximum values were not acting in the same plane, for each element to obtain the average shear. However, if the appropriate values of F_{xz} and F_{yz} (i.e., those acting in the same plane) are combined, it was found that the average value of F_{xz} is 132 kips/ft and the average value of F_{yz} is 106 kips/ft. As may be seen, these values are considerably less than 210 kips/ft, and are less than one-half of the shear capacity of 274 kips/ft.

(b) The above values represent the shear at a point. If an average shear is calculated along an east-west line running between column lines R and Q from the containment to the exterior of the mat using the HEA and EBASCO (ESI) computer runs, the following results are found:

	HEA	ESI
DBE (with load combinations)	103 k/ft	127k/ft
Normal (with load combinations)	66 k/ft	65 k/ft

Once again it may be seen that the shear stresses are much less than one-half of the shear capacity of 274 kips/ft. In addition, based on the discussion in section II of this report, it can be estimated that the maximum additional shears that can be developed from differential settlement of the base mat, even when postulating a gross difference (2:1) in soil stiffness under adjacent blocks, are calculated to be on the order of about 16 kips/ft. Thus, the developed shear stresses will still be small as compared to the shear capacity of the mat.

It should be noted, as discussed in section 8 of this report, that large triangular finite elements were used by the applicant to model the mat and its associated structures. The use of these elements produces sharp variations in computed moments and shears from element to element. Because of these variations, BNL's evaluation looked at average values for these forces, derived from several sets of adjacent elements, in order to arrive at representative values.

14. Vertical Wall Cracking

The shield wall is very stiff as compared to the basemat because of its wall thickness and circular geometry. It is therefore unlikely that the differential settlement of the basemat could have developed the cracks in the shield wall. In our opinion, these cracks must have been caused by thermal and shrinkage effects which occurred after the concrete placement.

Cracks have also been observed in other vertical walls such as those at the cooling tower. These walls are not as stiff as the shield wall since they are plane. Therefore, it would be possible for these cracks to have been caused by the differential movements of the basemat in addition to thermal and shrinkage effects. It is our opinion that the cracks in these walls occurred during construction when the basemat was subjected to its largest differential settlements. Now that the long term settlements have stabilized, these cracks are not expected to grow.

A more refined analysis, considering the actual configuration of the plant during various stages of construction, would provide the quantitative basis for determining the origin of the vertical wall cracks. However, it is concluded that these cracks do not appear to raise a significant safety issue.

CONCLUSIONS AND RECOMMENDATIONS

(a) The Waterford plant is primarily a box-like concrete structure supported on a 12-foot thick continuous concrete mat which houses all Class 1 structures. The plant island is supported by relatively soft overconsolidated soils. To minimize long term settlement effects, the foundation mat was designed on the floating foundation principle. The average contact pressure developed by the weight of the structure is made approximately equal to the existing intergranular stresses developed by the weight of the soil overburden at the level of the bottom of the foundation mat. Thus, net changes in soil stresses due to construction and corresponding settlements can be anticipated to be relatively small.

(b) In reviewing the information, reports, and computer outputs supplied to BNL by EBASCO, HEA, and LP&L, it is concluded that normal engineering practice and procedures for the analysis of nuclear power plant structures were employed.

(c) Accepting the information supplied to BNL pertaining to loadings, geometries of the structures, material properties and finite element mesh data, it is our judgment that:

(i) the bottom reinforcement as well as the shear capacity of the base mat are adequate for the loads considered.

(ii) the computed dead weight output data can be used to explain the pattern of cracking that has appeared on the top surface of the mat. The cracks that appear probably occurred after construction of much of the superstructure but before placement of all of the backfill and restoration of the ground water to its natural level. Growth of the cracks would then have been constrained by subsequent backfill soil and water pressures.

(iii) The cracks that have appeared in the vertical walls of structures placed on the base mat do not affect the conclusions regarding the strength of the base mat and do not appear to present a significant safety issue.

(d) It is recommended that a surveillance program be instituted to monitor the cracks, water leakage and chemical content of the water on a regular basis.

(e) BNL has reviewed the information and analyses provided by EBASCO, HEA, and LP&L. Those analyses could be refined in the following areas:

(i) dynamic coupling between the reactor building and the base mat for seismic stresses resulting from the vertical earthquake input (see section 5);

(ii) dynamic effects of lateral soil/water loadings (see section 6);

(iii) artificial boundary constraints in finite elements models (see section 7);

(iv) fineness of base mat element mesh (see section 8);

(v) origin of cracks in the vertical walls (see section 14).

Based upon our approximate calculations together with engineering judgment, we do not anticipate that the refinement of these analyses will lead to major changes in calculated stress levels; nonetheless, it is recommended that the detailed confirmatory calculations mentioned above be performed. For all of these reasons it is our conclusion that the safety margins in the design of the base mat are adequate.

APPENDIX A

LIST OF CONTRIBUTORS

Listed below in alphabetical order are the names of the contributors to this report:

Costantino, C. J.

Miller, C. A.

Philippacopoulos, A. J.

Reich, M.

Sharma, S.

Wang, P. C.

Appendix B

Stresses Induced While Pouring Blocks

A question has been raised concerning the stresses which could have been introduced when the basemat blocks were being poured. The response of two adjacent blocks during construction are considered. The first block is taken to be in place when the second block is placed. It is also assumed that the concrete in the second block hardens immediately so that it can transmit loads to the first block. The subgrade modulus under the two blocks is assumed to be different so that the effect of soft spots in the soil can be considered. A sketch of the problem to be considered is shown in Fig. B1.

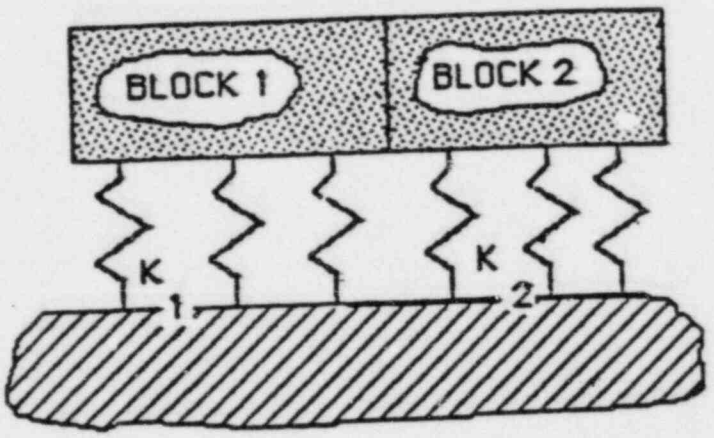

Fig.B1 Construction of Two Adjacent Blocks

When the first block is poured it settles an amount,

$$\Delta_1 = W/K_1$$

The second block is then poured. If the concrete is conservatively assumed to harden before the soil settlement can occur, the second block

will introduce additional loadings on the first block. The new deformation caused by the weight of the second block is shown on Fig. B2.

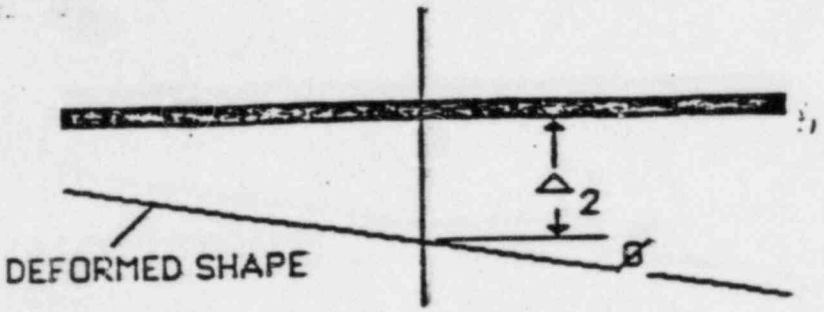

Fig.B2 Deformed Shape of Blocks

The loads acting on the block may then be determined by multiplying the deformations by the foundation moduli. These loads are shown on Fig. B3.

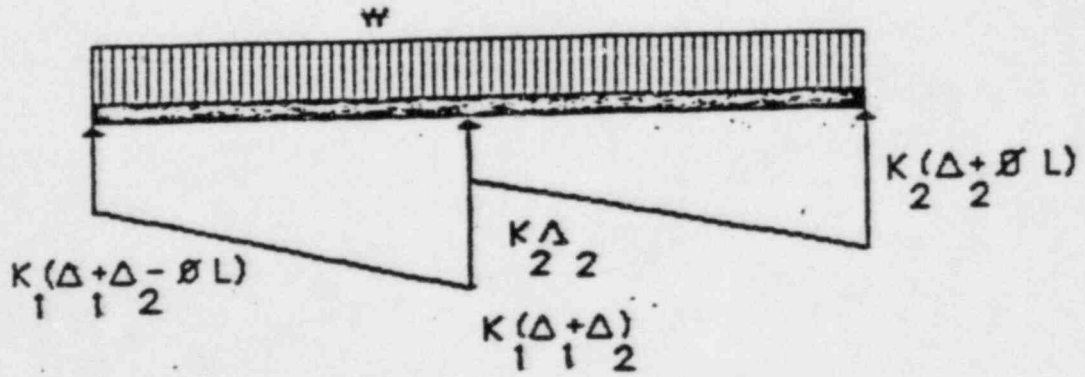

EigB3 Loads Acting on Blocks

Force and moment equilibrium allow the two unknown displacements (Δ_2, ϕ) to be calculated. The results are,

$$\Delta_2 = W\,[7 + \delta_b)/(I + 14\delta_b + \delta_b^2)]/K_1$$

$$\phi = 12\,W/LL\,K_1\,(I + 14\delta_b + \delta_b^2)]$$

where, $\delta_b = K_2/K_1$

Once the displacements are known the loads on the blocks may be evaluated and beam shears and bending moments may be computed. This is done for foundation moduli ratios of 1 and 0.5. Peak values of shear and moment are tabulated in Table BI.

Table BI

Shear and Moments in Blocks During Construction

Foundation Moduli Ratio ( )	Maximum Shear (Kips/ft)	Maximum Moment (Kip-ft/ft)	Required f'c (psi) to Prevent Shear	Required f'c (psi) to Prevent Bending Tension
1	11	101	15	15
0.5	16	275	31	113

For the design concrete strength of 4000 psi, the shear capacity of the concrete section is 274 kips/ft. As may be seen this is much larger than the peak shears that could be caused during construction. Bending cracks will occur in the concrete when the peak concrete tensile stress

reaches the modulus of rupture. For the concrete design strength this will occur at a bending moment of 1640 kip-ft/ft. It may be seen that the peak moments are closer to the value required to cause a bending crack than the peak shears are to the value required to cause a diagonal tension crack.

The concrete will not have attained its final strength at the time when these stresses occur. The last two columns in Table B1 list the required concrete compressive strength to prevent shear and moment failures. Two conclusions may be drawn from these data. First, even for rather dramatic variations in foundation moduli, only a minimal concrete strength is required to present either a shear or moment crack. Second, if a crack were to develop it would most likely be a bending crack.

The above analysis is based on the assumption that the concrete hardens before soil settlement occurs. If this were not so, the wet concrete would fill the void volume created by soil settlement. The concrete block would then be supported on the soil rather than "hanging" from the other block. Figure B4 shows the concrete strength gain during the first day. As may be seen concrete will have no strength until about 8 hours. By this time all of the soil settlement would have occurred and the second concrete block would not induce any loads on the first block.

Fig. B4 From: "Concrete" by S. Mindess, J. T. Young, Prentice Hall

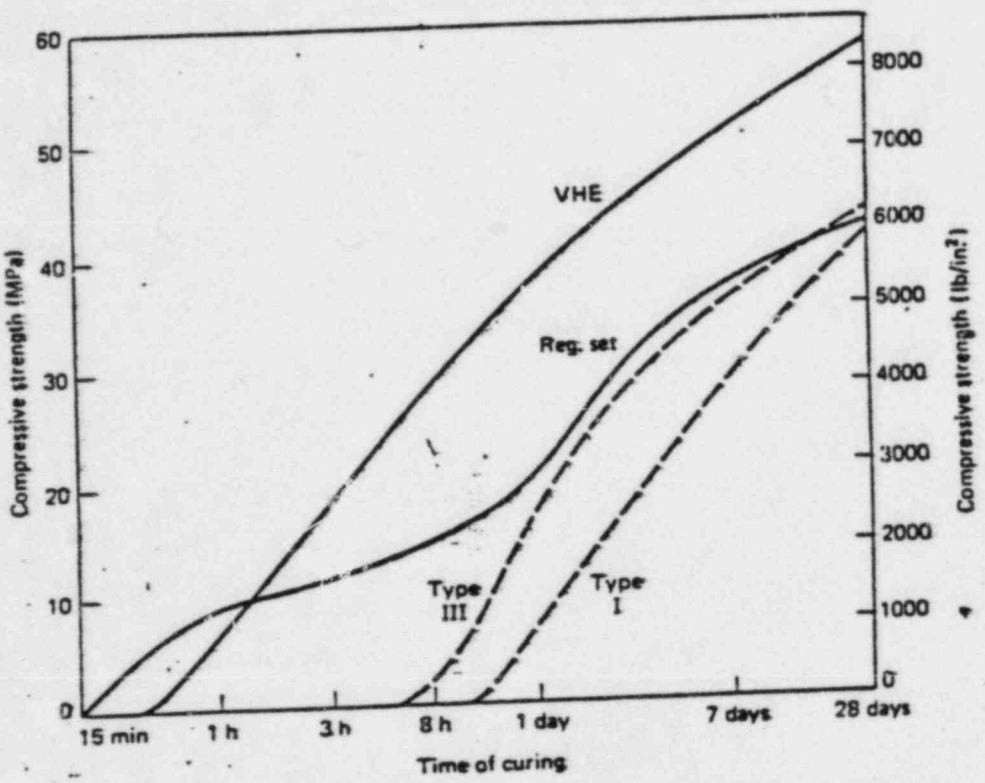

Figure 3.13 Strength developments of concretes made with rapid-hardening cements. (Adapted from W. Perenchio, in *New Materials in Concrete Construction*, ed. S. P. Shah, University of Illinois at Chicago Circle, Chicago, 1972, p. 12–VI.)

placement and have the advantage of better water resistance. But the very rapid strength gain of the cement suggests many other applications in which the properties of a portland cement are desired: pavement and bridge-deck repair, precasting operations, shotcreteing, and slip forming. It is unfortunate that regulated-set cement is not currently available in the U.S., but the interesting properties of the cement will no doubt ensure its reappearance.

VHE Cement

In the production of VHE cement, calcium sulfate is added to the raw mix so that $C_4A_3\overline{S}$ is formed in the rotary kiln. This is the same compound that is present in Type K expansive cements, but the quantities are greater in VHE cement. Calcium sulfate ($C\overline{S}$, insoluble anhy-

Appendix C

Effect of Sidewall Loads On Basemat Capacity

Soil pressure loads act on the sidewalls and these loads introduce compressive stresses in the slab of the basemat. This compressive stress will assist in resisting the diagonal tension stresses which occur in the slab. The significance of this effect is discussed in this Appendix.

Table CI lists the horizontal loads which act on the sidewalls due to the various load combinations. These loads were determined directly from the HEA/Ebasco computer printouts.

Table CI.

Total Force Acting on the Wall Surface (kips)

Load Case	Wall #1	#2	#3	#4
Case 4: Normal Soil Pressure	36619	36441	50942	50522
Case 8: SSE & Soil (North to South)	27061	110657	50684	50377
Case 10: SSE & Soil (South to North)	111051	26907	50684	50377

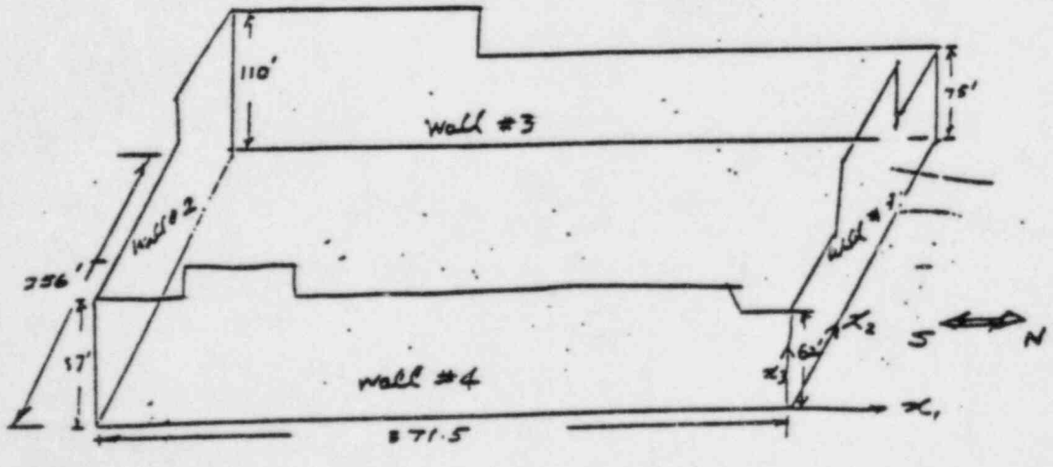

An elevation of the structure parallel to the long direction of the basemat is shown on Fig. C1.

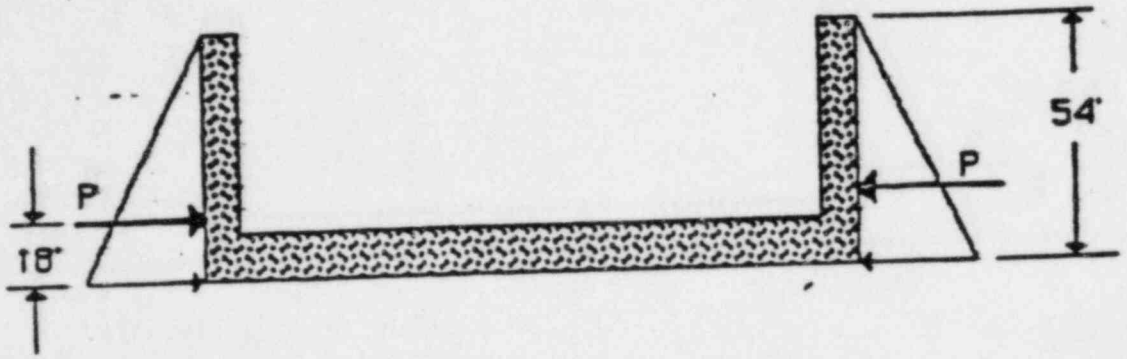

Fig.C1 Estimated Side Loads On Wall

The forces (P) are taken as the forces shown on Table C1 and acting on walls #2 and #4. The soil pressure is assumed to have a triangular variation as shown so that the resultant force (P) acts at the third point on the wall. Since the wall is buried about 54', the resultant force acts at a point 18' up the wall from the bottom of the basemat.

The stresses caused by this loading in the cross section are shown on Fig. C2.

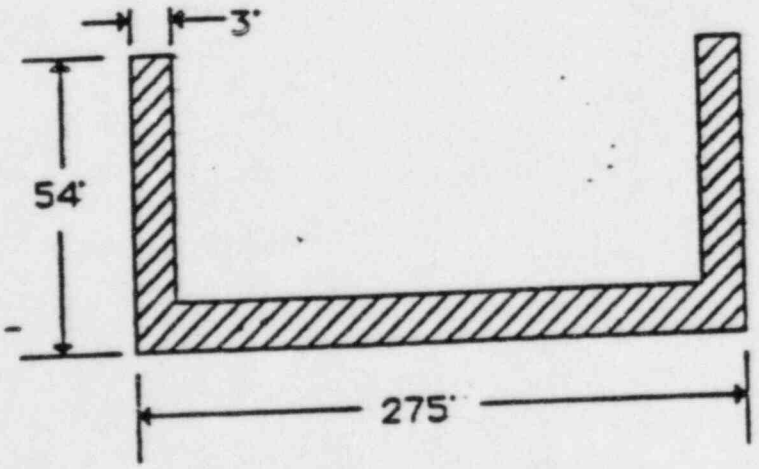

Fig.C2 Cross Section of Basemat

The basemat is analyzed as a beam structure. The cross section shown in Fig. C2 has the following properties:

Cross sectional area = 3552 square feet

Centroid at 7.91' above the bottom of the mat

Moment of Inertia = 247300 feet ^{4}

Stresses are then computed as:

$$f = P/A \pm M z / I$$

Therefore at the top of the wall,

$$f_{tw} = P/3552 + P (18-7.91) (54-7.91) / 247300$$

The stress at the top of the slab is,

$$f_{ts} = P.3552 - P (18-7.91) (12-7.91) / 247300$$

The stress at the bottom of the slab is,

$$f_{bs} = P.3552 - P (18-7.91) (7.91) / 247300$$

The resultant stresses for the Case 4 loads (Normal soil pressure) are:

f_{tw} = 541 psi

f_{ts} = 112 psi

f_{bs} = -11 psi

The stresses for Case #8 (SSE in N-S) are:

f_{tw} = 465 psi

f_{ts} = 84 psi

f_{bs} = -8 psi

The average stresses in the slab for these two load cases are 51 psi and 38 psi respectively. The average shear in the basemat for the vertical shear loadings (see section 9) was found to be 50 psi. If this shear stress is combined with the 38 psi average compressive stress one finds that the diagonal tensile stress in the concrete is reduced to 34 psi. It is unlikely that this stress could cause a shear (diagonal tension) failure given the 107 psi shear capacity.